

# CLASSIFIER FUSION OF POLSAR, HYPERSPECTRAL AND PAN REMOTE SENSING DATA FOR IMPROVING LAND USE CLASSIFICATION

R. Saadi<sup>1</sup>, M. Hasanlou<sup>1,\*</sup>, A. Safari<sup>1</sup>

<sup>1</sup> School of Surveying and Geospatial Engineering, College of Engineering, University of Tehran  
(ramin.saadi, hasanlou, asafari) @ut.ac.ir

Commission VI, WG VI/4

**KEY WORDS:** Classification, Hyperspectral, Land cover, PolSAR, Polarization signature, Fusion

## ABSTRACT:

The combined use of PolSAR and hyperspectral data can improve the classification accuracy. This paper proposes a new classification approach for combining use of PolSAR and hyperspectral image data sets. At the first step, polarization signature is generated from coherency matrix of PolSAR image data. In the second step, in order to improve spatial resolution, the Hyperion image was pan-sharped with the ALI Pan image. In the third step, the Random Forest (RF) classifier is used for classifying PolSAR and hyperspectral data sets in five different classes including: Water (Wa), urban area (Ur), vegetation (Vg), road (Ro), and soil (So). Then, in order to fuse the output of RF for incorporated two data sets, simple majority voting (MV) and weighted majority voting (WMV) methods are used. Three UAVSAR, Hyperion and ALI images that acquired on April 2015 was chosen for this study. The results showed the ability of the polarimetric data for classifying urban and vegetation, and hyperspectral images for water, soil and road classes. Also, the combination of two data sets by using of WMV method causes the improvements of the classification performance.

## 1. INTRODUCTION

Land use/cover information plays an important role in environmental assessment, planning and management in regional development. Remote sensing images play an important role in providing information about land use/cover (Foody, 2002). For each pixel in a hyperspectral image, a continuous spectrum is sampled that can be used to identify different objects by the reflection of that object. One of the limitations of hyperspectral images is that it provides no surface penetration (Bordbari, et al. 2015). In order to overcome this limitation and improve the efficiency of hyperspectral imaging system and improve the classification accuracy, the combination of polarimetric SAR (PolSAR) and hyperspectral data is carried out. Microwaves used in radar images have the potential to penetrate the surface (especially the foliage and tree canopy) and interact with the surface below it, as well as provide information on the geometry and dielectric properties of the target (jafari, et al. 2015), and hyperspectral images provide information from the surface of the target (Borghys, et al. 2007). Thus, it is possible to identify two complementary data types. Thus, the combination of PolSAR and hyperspectral data can increase the ability to identify and classify land use/cover classes.

## 2. STUDY AREA AND DATAS ET

The study area is located in San Francisco city in United states. Three UAVSAR, Hyperion and ALI images that acquired on April 2015 are used for this study. Figure 1, illustrated a subset of Pauli color composite image, color composition of Hyperion image and panchromatic band of ALI.

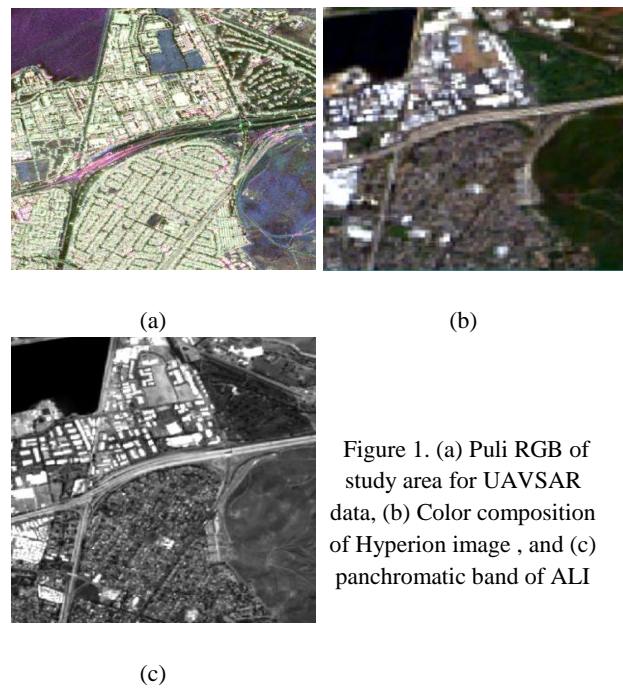


Figure 1. (a) Pauli RGB of study area for UAVSAR data, (b) Color composition of Hyperion image, and (c) panchromatic band of ALI

Table 1 and Table 2 shows the characteristics of the EO-1 and UAVSAR satellite data.

**Table 1.** The characteristics of the EO-1 satellite.

EO-1	ALI-PAN	Hyperion
------	---------	----------

\* Corresponding author

Spectral cover ( $\mu\text{m}$ )	0.48-0.69	0.35-2.5
Number of bands	1	242
Spatial resolution (m)	10	30
Spectral resolution	-	10

**Table 2.** The characteristics of the UAVSAR satellite.

Parameter	Value
Frequency	1.26 GHz (0.2379 m)
Bandwidth	80 MHz
Pulse Duration	5-50 $\mu\text{s}$
Polarization	Quad Polarization
Range Swath	16 Km
Look Angle Range	25° – 65°
Transmit Power	3.1 KW
Antenna Size	0.5m $\times$ 1.6 m
Operation Altitude Range	2000-18000 m
Ground Speed Range	100-250 m/s

Table 3 shows a set of classes with the numbers of training and testing samples, including the five various land cover classes, containing urban area, water, soil, vegetation, and road.

**Table 3.** Unsupervised threshold selection methods.

Name	# of train sample	# of test sample
Urban (Ur)	1796	898
Water (Wa)	978	489
Road (Ro)	2256	1128
Vegetation (Vg)	466	233
Soil (So)	686	343
Total	6182	3091

### 3. METHODOLOGY

The method used in this paper consists of five basic steps: (1) Pre-processing of three PolSAR, Hyperspectral, and ALI images. (2) Extracting the polarimetric signature. (3) Pan-sharpening (fusing) of Hyperion and ALI images. (4) Performing the RF classification. (5) Fusing the output of two PolSAR and Hyperspectral data by MV and WMV classifier fusion.

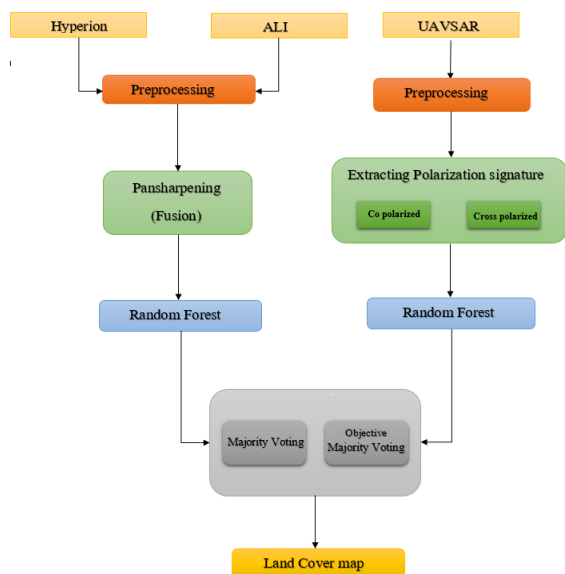


Figure 2. Flowchart of proposed method

#### 3.1 Pre-processing

To reduce the speckle noise in UAVSAR image, a box filter with 3 $\times$ 3 dimensions is used. For Hyperion images, firstly bands with low signal-to-noise ratio were removed. Then, the defective columns of the image were replaced with the mean values of adjacent column. Finally, FLAASH atmospheric correction was used to eliminate atmospheric effects. The next step is, image co-registration: Image co-registration is the process of geometrically aligning two or more images to integrate or fuse corresponding pixels that represent the same objects. To make it possible to combine two datasets, both must have the same spatial resolution. For this purpose, the spatial resolution of both images has been changed to 10.0 meters. The spatial resolution of the UAVSAR image was reduced to 10.0 m using resampling. On the other hands, the Hyperion image, which has a spatial resolution of 30.0 meters (after pan-sharpening with panchromatic band of ALI (Section 3.3)) improved to 10.0 m spatial resolution.

#### 3.2 Polarization signature

Polarimetric signature is a three-dimensional representation that demonstrates the polarimetric information. Two dimensions relate to polarization ellipse geometric parameters. ellipticity- $\tau$  and orientation angles- $\varphi$ . The third dimension also relates to the target's response (Van Zyl, et al 1987). Generally, the back scattering of the target is the function of two polarizations: incident and backscattered polarizations. If polarization of the incident and backscattered wave is the same, polarimetric signature is obtained in co-polarized state, and if two polarizations are perpendicular to each other, polarimetric signature is obtained in cross-polarized state (Van Zyl, et al 1987). The scattering matrix is used to describe and analysis of backscattering of pure and coherent targets. But for the real targets, who's their backscattering is a partial polarize, using the scattering matrix for the analysis is difficult. Hence, the second order descriptors that extracted by scattering matrix is employed to increase information extraction and reducing the errors (Nasr and Abdelhamid, 2016). The coherency matrix which their elements are directly related to physical properties of the targets is chosen instead of scattering matrix Eq. (1):

$$T = \begin{bmatrix} (S_{hh} + S_{vv})(S_{hh} + S_{vv})^* & (S_{hh} + S_{vv})(S_{hh} - S_{vv})^* & 2(S_{hh} + S_{vv})S_{hv}^* \\ (S_{hh} - S_{vv})(S_{hh} + S_{vv})^* & (S_{hh} - S_{vv})(S_{hh} - S_{vv})^* & 2(S_{hh} - S_{vv})S_{hv}^* \\ 2S_{hv}(S_{hh} + S_{vv})^* & 2S_{hv}(S_{hh} - S_{vv})^* & 2S_{hv}S_{hv}^* \end{bmatrix} \quad (1)$$

$$= \begin{bmatrix} 2(A_0) & (C) - j(D) & (H) + j(G) \\ (C) + j(D) & (B_0) + (B) & (E) + j(F) \\ (H) - j(G) & (E) - j(F) & (B) - (B_0) \end{bmatrix}$$

where  $v$  and  $h$  represent the vertical ( $\tau = 0^\circ$ ,  $\varphi = 90^\circ$ ) and horizontal ( $\tau = 0^\circ$ ,  $\varphi = 0^\circ$ ) polarization basis, respectively. The  $S_{hv}^*$  is the conjugated of  $S_{hv}$ . according to (Lee and Pottier, 2009) and (jafari, et al. 2015), to generate the polarimetric signature form coherency matrix, firstly the  $k$  matrix is calculated through Eq. (2).

$$k = \begin{bmatrix} A_0 + B_0 & C & H & F \\ C & A_0 + B & E & G \\ H & E & A_0 - B & D \\ F & G & D & -A_0 + B \end{bmatrix} \quad (2)$$

The equation (3) is used to compute the backscattered powers in different polarization basis for both co-polarization and cross polarization.

$$P_{\phi,\tau} = V_{re}^t [K] V_{tr} \quad (3)$$

where  $V$  can be computed from Eq. (4) for both transmission and receive modes.

$$\vec{V} = \begin{bmatrix} V_0 \\ V_1 \\ V_2 \\ V_3 \end{bmatrix} = \begin{bmatrix} 1 \\ \cos 2\tau \cos 2\phi \\ \cos 2\tau \sin 2\phi \\ \sin 2\tau \end{bmatrix} \quad (4)$$

Eq. (3) is used to compute the polarimetric signature in two co-polarized ( $V_{tr} = V_{re}$ ) and cross-polarized ( $V_{tr} = V_{re}^\perp$ ) cases, in which the values of  $\tau$  and  $\phi$  are in the range 0:180 and -45:45, respectively. The polarimetric signature for Trihedral in Co and Cross polarized cases are shown in Figure 3.

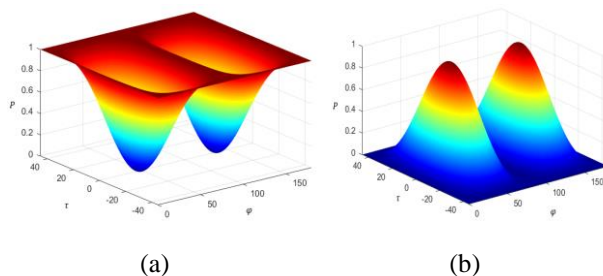


Figure 3. Polarization signature for Double Bounce. (a) co-polarized (b) cross-polarized

### 3.3 Pan-sharpening (fusing) of Hyperion and ALI images

One of the most important processes used in remote sensing is data fusion. In general, fusion in remote sensing is always done to improve data quality and increase the performance of analyzes. usually in remote sensing image fusion, information from two different sensors is shared. Fusion in remote sensing is performed on three levels (Seydi, Hasanlou 2018): (1) Pixel level, (2) Feature level, and (3) Decision level. One of the most important techniques for pixel-level fusion is the Pansharpening technique (Yokoya, et al. 2017). This technique is a fusion of a panchromatic image and a multi-spectral or hyperspectral image that is simultaneously provide from a region. The purpose of this fusion is to combine the spatial detail of the panchromatic image (which is not in the hyperspectral image) with the spectral bands of the hyperspectral image (vs. single-band of panchromatic image). This paper proposes a new classification approach base on fusion of Hyperspectral and PolSAR images. The proposed method is a fusion in decision level. For this purpose, Hyperion and UAVSAR images that used in this study, need to have the same spatial resolution. Hyperion image have a spatial resolution of 30.0 meters. The Panchromatic band of ALI, which has a spatial resolution of 10.0 meters has been used to improve the spatial resolution of Hyperion. After fusing PAN image of ALI with Hyperion data, a high-resolution spectral that also has a spatial resolution of 10.0 meters is made. According to 3.1, UAVSAR image also has a spatial resolution of 10.0 m, and two data sets are ready to be fused.

### 3.4 Random Forest

Random forest (RF) is a supervised classification method that is based on multiple decision trees during the training of the

algorithm, which is the output of each decision tree is considered as one class (Breiman, 2001). RF classification uses random or combination features of each sample to grow a tree. Each sample (pixel) is assigned to a class that has the maximum votes among all voters (classifier trees) (Breiman, 2001). The number of features used per pixel to construct a tree and the number of trees that need to grow are two user-defined parameters for constructing a random forest classification. For each pixel, only the selected features are searched for the best division. Therefore, the classification of a random forest consists of  $N$  trees, where  $N$  is the number of trees that grow, and these trees can have any defined value by the user. To classify a new data set, each item in the data set is passed to each of  $N$  trees. The forest, chooses the class with the highest number of votes from the  $N$  trees (Pal, 2005).

### 3.5 Objective Majority Voting

One of the simplest methods to combine the outputs of several classification algorithms is majority voting (MV). (Kuncheva, 2014). Majority counts the number of votes per class for entries and select the class with the maximum votes (Orrite, et al. 2008). There may be some ambiguity in the MV method (Khosravi, et al. 2017): First, two or more classes have the highest number of votes. Second, none of the classes has the highest number of votes. Due to the above problems, MV cannot decide explicitly for all samples. In order to solve this ambiguity, a weighted majority voting (WMV) method has been used to develop the MV method as follows:

- (1) When the number of votes for a class is greater than or equal to  $\frac{n}{2} + 1$  ( $n$  is equal to the number of decision trees) or, when the number of votes in a class is maximized, the WMV will become a simple MV method.
- (2) When the number of votes is equal to two or more classes, the WMV makes a decision based on the ratio between producer accuracy and user accuracy as follows: if the sum of  $PA_i/UA_i$  ( $i$ : class index) is maximized.
- (3) When all classes have only one vote, OMV is based on overall accuracy. The class is the winner whose output has the highest overall accuracy.

## 4. RESULTS

Based on the methodology described above, the results are showed in Figure 4.

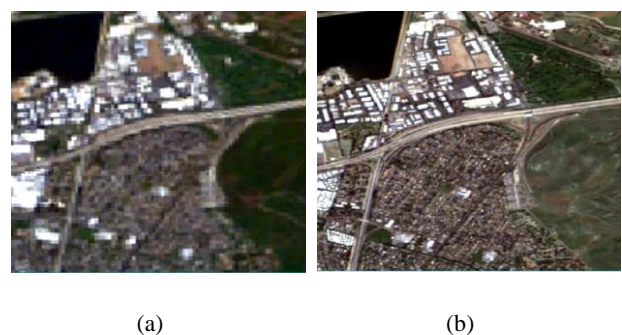


Figure 4. (a) Color composition of Hyperion image, (b) Pan-sharpened image

Overall Accuracy (OA) and Kappa coefficient (Congalton, 1991) derived from the RF classification in six, co-polarized signature, cross-polarized signature, the combination of co and cross polarized signature, hyperspectral, combination of polarimetry and hyperspectral with MV and WMV for the study area and for five class are presented in Table 4.

**Table 4:** Overall Accuracy (OA) and Kappa coefficient

	Co-polarized	Cross-polarized	Co & cross polarized	Hyper spectral	MV	WMV
<b>OA</b>	94%	92.6%	94.79%	96.44%	96.83%	98.41%
<b>Kappa</b>	91.99	89.98	92.96	95.54	95.70	97.86

Final confusion matrixes derived from the RF classification and Weighted Majority Voting method for the study area and for five class are presented in Table 5.

**Table 5:** Confusion matrix for WMV

	Ur	So	Wa	Ro	Vg	User accuracy
Ur	891	1	0	2	4	99.22%
So	14	467	0	8	0	95.50%
Wa	0	0	1128	0	0	100%
Ro	0	6	0	220	7	94.42%
Vg	2	1	0	4	336	97.95%
Overall accuracy						98.63%

Figure 5 illustrates the land cover map of study area that produced from proposed method.

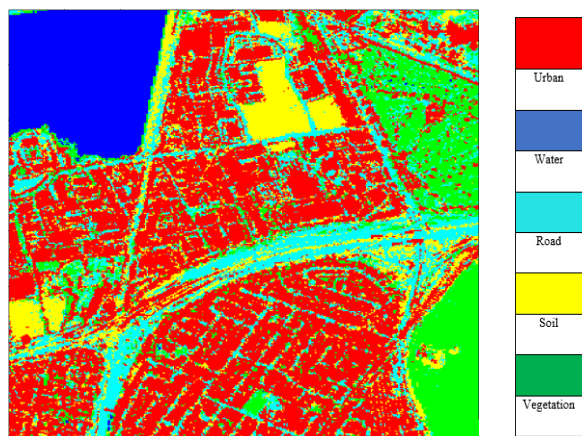


Figure 5. Land use map 1990 (b). Land use map 2018

## 5. CONCLUSION

This paper proposes a new classification approach for combined use of PolSAR and hyperspectral image and RF classification method. Analysing the ability of the polarimetric and hyperspectral data to identify and classify the various land cover classes shown the ability of the polarimetric data for classifying road and Soil, and hyperspectral images for water, urban and vegetation classes. Also, the combination of two data set by using of majority voting method causes the improvements of the classification.

## 6. REFERENCES

Breiman, L. (2001). Random Forests, Vol. 45. *Mach Learn*, 1.

Bordbari, R., Maghsoudi, Y. and Salehi, M., 2015. Detection of built-up areas using polarimetric synthetic aperture radar data and hyperspectral image. *International Archives of the Photogrammetry, Remote Sensing & Spatial Information Sciences*, 40.

Borghys, D., Shimoni, M., Degueldre, G. and Perneel, C., 2007, April. Improved object recognition by fusion of hyperspectral and SAR data. In *Proceedings 5th EARSeL Workshop on Imaging Spectroscopy. Bruges* (Vol. 1).

Congalton, R.G., 1991. A review of assessing the accuracy of classifications of remotely sensed data. *Remote sensing of environment*, 37(1), pp.35-46.

Foody, G.M., 2002. Status of land cover classification accuracy assessment. *Remote sensing of environment*, 80(1), pp.185-201.

Jafari, M., Maghsoudi, Y. and Zoj, M.J.V., 2015. A new method for land cover characterization and classification of polarimetric SAR data using polarimetric signatures. *IEEE Journal of Selected Topics in Applied Earth Observations and Remote Sensing*, 8(7), pp.3595-3607.

Khosravi, I., Safari, A., Homayouni, S., & McNairn, H. (2017). Enhanced decision tree ensembles for land-cover mapping from fully polarimetric SAR data. *International journal of remote sensing*, 38(23), 7138-7160.

Kuncheva, L. I. (2014). *Combining pattern classifiers: methods and algorithms*. John Wiley & Sons.

Lee, J.S. and Pottier, E., 2009. *Polarimetric radar imaging: from basics to applications*. CRC press.

Nasr, A.H. and Abdelhamid, H.Z., 2016. Polarimetric Signatures Identification for Different Features in Radarsat-2 PolSAR Image: A Case Study of Halayib Area, Egypt. *The International Archives of Photogrammetry, Remote Sensing and Spatial Information Sciences*, 41, p.851.

Orrite, C., Rodríguez, M., Martínez, F., & Fairhurst, M. (2008, September). Classifier ensemble generation for the majority vote rule. In *Iberoamerican congress on pattern recognition* (pp. 340-347). Springer, Berlin, Heidelberg

Pal, M. (2005). Random forest classifier for remote sensing classification. *International Journal of Remote Sensing*, 26(1), 217-222.

Pal, M. (2005). Random forest classifier for remote sensing classification. *International Journal of Remote Sensing*, 26(1), 217-222.

Seydi, S. T., & Hasanlou, M. (2018). Sensitivity analysis of pansharpening in hyperspectral change detection. *Applied Geomatics*, 10(1), 65-75.

Van Zyl, J.J., Zebker, H.A. and Elachi, C., 1987. Imaging radar polarization signatures: Theory and observation. *Radio science*, 22(04), pp.529-543.

Yokoya, N., Grohnfeldt, C., & Chanussot, J. (2017). Hyperspectral and multispectral data fusion: A comparative review of the recent literature. *IEEE Geoscience and Remote Sensing Magazine*, 5(2), 29-56.